Proceedings of the Reactor Physics Asia 2023 (RPHA2023) Conference
Gyeongju, Korea, October 24-26, 2023

Preliminary neutronics and thermal analysis of a heat pipe cooled traveling wave reactor with nonuniform radial fuel arrangement

Kunfeng Ma [a], Po Hu [a*]
[a] *School of Nuclear Science and Engineering, Shanghai Jiao Tong University, Shanghai 200240, China*
[*] *Corresponding author: pohu@sjtu.edu.cn*

Abstract

This paper presents a heat pipe cooled traveling wave reactor (HPTWR) with nonuniform radial fuel arrangements for energy supply of decentralized electrical market. The reactor adopts neutron traveling wave to pursue the high breeding capability. To reduce the highest operation temperature of nuclear fuel, the HPTWR is divided into three fuel regions in radial direction. Burnup calculations of reactor and thermal analysis of heat pipe (HP) were performed using Monte Carlo code RMC and thermal resistance-capacitance network model (TReCan). Results show the 70 MW_{th} HPTWR with nonuniform radial fuel arrangements can continuously operate 50 years with 0.7% reactivity swing. The highest operate temperatures of UN fuel and HP wall in the HPTWR with nonuniform radial fuel arrangement are about 2345 K and 1774 K respectively at BOC. The corresponding highest operate temperatures of UN and HP wall are decreased to about 2235 K and increased to about 1782 K respectively at EOC.

1. Introduction

As one of the Small Modular Reactors (SMRs), heat pipe reactor (HPR) is a new type of reactor, which uses alkali metal heat pipes (HPs) to export the fissile heat out of the core [1]. Compared with the traditional primary loop layout, HPR does not need pumps and pipes, which has compact structures, light weight, and high safety [2]. Therefore, HPR possesses good mobility and plugplay availability, and is particularly attractive to decentralized electrical markets.

The concept of HPR was first proposed by Los Alamos National Laboratory (LANL) in 1960s, which was originally designed to provide power sources for space exploration [3]. Recently, a series of high power HPRs have been proposed to achieve the energy supply of the decentralized electrical markets [4-7]. In 2015 years, LANL [4] proposed a 5 MW_{th} Megapower reactor, which mainly consists of stainless steel monoliths, UO_2 fuel, HPs and Al_2O_3 reflector. The lifetime of reactor is higher than 12 years in the case of full power output. Then, Westinghouse [5] proposed a 15 MWe eVinci reactor in 2017 years. The reactor consists of a stainless cylinder monolith, HPs, fuel pins, reflector, and metal hydride moderator. The core with the low enriched uranium can operate for more than 10 years without refueling. Recently, a 65.5 MW_{th} heat pipe coolant traveling wave reactor (HPWTR) has been proposed in our previous works [6]. The reactor consists of 1008 fuel elements in the radial direction, and ignition fuel region and breeding fuel region in the axial direction. The solid monolith will be not used in the HPTWR because it has a higher thermal stress during the reactor operation and complexity in manufacturing. The HPWTR can operate for 59 years without refueling. Then, the heat transfer capability of HP was assessed and the HPTWR design is optimized. In the optimized HPTWR, the length of breeding fuel region is increased to about 70 cm and the cladding is replaced by the Mo-14Re relative to original HPTWR. Results show the optimized HPTWR can achieve 70 MW_{th} power output and 46 years continuous operation [7].

The UN fuel and HP wall in the highest power fuel element for the optimized HPTWR have relatively higher operation temperatures, which are about 2394 K and 1800 K respectively at beginning of cycle (BOC) [7]. To reduce the highest operation temperatures of fuel and HP wall, the fuel element will be divided into three fuel regions in the radial direction and the corresponding radial power peak factor will be reduced. Besides, the radial nonuniform radial fuel arrangement technology has been applied various heat pipe reactor, such as yttrium hydride moderated micro heat pipe reactor [8] and HP-STMCs [9]. Section 2 describes the core geometry and computational tool. Section 3 presents the results of depletion. Section 4 gives the conclusions.

2. Core design and computational tool

2.1 Core design

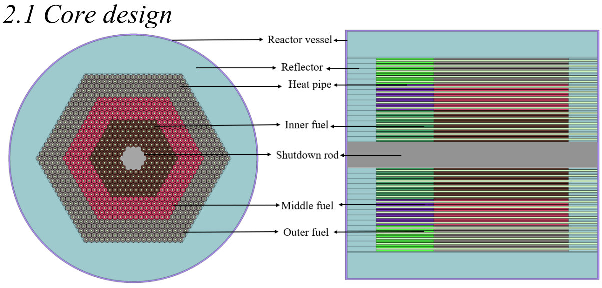

Fig.1 Radial and axial cross-section views of RMC model of HPTWR with nonuniform radial fuel arrangement

Fig.1 shows the schematic diagram of the HPTWR with nonuniform radial fuel arrangement. The reactor consists of three fuel regions in the radial direction and two fuel regions in the axial direction. The ^{235}U enrichments in the radial inner fuel region, middle fuel region and outer fuel region increase in turn to reduce the radial power peak factor. The reactor consists of 198 inner fuel regions, 330 middle fuel regions and 480 outer fuel regions (total 1008 fuel elements). Besides, the reactor consists of ignition fuel region and breeding fuel regions in the axial direction. Therefore, the reactor consists of six fuel regions. Table 1 shows the ^{235}U enrichments of UN fuel in every fuel region. The geometry parameters of fuel element and HP have been showed in our previous work [7]. The HPTWR with nonuniform radial fuel arrangement, including the radial and axial Al_2O_3 reflectors, are 90.3 cm radius and 130 cm long. The main design parameters of reactor are described in Table 2.

Table 1 Fuel enrichments of every region for HPTWR with nonuniform radial fuel arrangement

Region	Inner fuel region	Middle fuel region	Outer fuel region
Ignition fuel region	12.97%	13.92%	14.87%
Breeding fuel region	9.07%	10.02%	10.97%

Table.2 Main parameters for HPTWR with nonuniform radial fuel arrangement

Parameters	Value	Parameters	Value
Power (MW_{th})	70	Fuel cladding material	Mo-14Re
Total number of fuel elements	1008	Density of Mo-14Re (g/cm^3)	12
Element to element pitch (cm)	3.8256	Total number of HPs	1008
Fuel	UN	^{7}Li enrichment in HP (%)	99.9
^{15}N enrichment in fuel (%)	99.9	Density of Li (g/cm^3)	0.414
Density of fuel (g/cm^3)	13.59	Reflector material	Al_2O_3
Ignition fuel region length (cm)	30	Density of reflector (g/cm^3)	3.9
Breeding fuel region length (cm)	70	Side reflector outer radius (cm)	90.3
Mass of U (tons)	12.11	Radial reflector thickness (cm)	18.71-28.30
Density of He (g/cm^3)	0.000037	Axial reflector length (cm)	15
Safety rod channel outer radius (cm)	8	Temperature of reflector (K)	900

2.2 Computational tool

All the neutronics calculations of the HPTWR with nonuniform radial fuel arrangement are performed using the Monte Carlo program RMC, which is a probabilistic code developed by Tsinghua University [10-11]. The continuous-energy cross section based on the ENDF/B-VII library is used for the RMC calculations in this study [12]. Each depletion calculation in the reactor has 50 inactive cycles and 250 active cycles with 30,000 particle history per cycle. All the HPs, cladding and UN fuel have a same operational temperature (1700 K) in the neutronics calculations. The core is equally divided into 20 smaller zones in the axial direction to simulate the axial neutron breeding wave of the reactor in the depletion calculation [13-14].

The heat calculations of HPs in the HPTWR with nonuniform radial fuel arrangement are performed using thermal resistance-capacitance network model (TReCan), which has been verified in our previous work [7]. The axial power distribution of fuel element can be obtained by the RMC code. The evaporation section of HP is also divided into 20 small zones in the thermal analysis, which is same to that in the neutronics calculations. The fission power of fuel element is added into the evaporation section of HPs in the thermal analysis. The condensation section of HP is cooled by liquid metal Li because it has a higher heat transfer capability under the higher operational temperature. The operate temperature and velocity of liquid metal Li in the condensation section of HPs are assumed to be 1590 K (the boiling point of liquid Li is about 1613 K) and 0.3 m/s respectively. Under $10^4 < \mathrm{Re} < 10^5$, the Nusselt number for Li coolant surrounding the cylinder can be estimated with correlation

$$\mathrm{Nu} = 8 + 0.002 \times \mathrm{Re}^{0.8} \text{ [15]} . \quad (1)$$

The heat transfer between the intermediate coolant and HP wall can be calculated by the Newton's law of cooling, which can be showed by

$$\mathrm{Q} = \frac{\mathrm{Nu} \times K_{cool}}{L_{cool}} \times S_{cool} \times (\mathrm{Tw} - \mathrm{Tc}). \quad (2)$$

Where the S_{cool}, Tw and Tc are the surface area of condensation HP wall, temperature of liquid metal Li and temperature of HP wall respectively. The length of adiabatic, and condensation sections for Li HP are set to be 0.35 m and 1.0 m respectively.

3. Results

3.1 Burnup of reactor

To investigate the effect of divided radial fuel regions to the reactor reactivity, the fuel burnup calculations first are performed. Fig.2 shows the time profiles of k_{eff} for HPTWR with nonuniform radial fuel arrangement and optimized HPTWR. The initial k_{eff} of HPTWR with nonuniform radial fuel arrangement is about 1.0015 and then gradually increases to about 1.007 at about 30 years because the positive reactivity inserted by the new bred fissile nuclides (mainly ^{239}Pu and ^{241}Pu) in the reactor is higher than the negative reactivity by the accumulation of produced fission products and consumed nuclear fuel. Then, the k_{eff} gradually decreases during the next operation because a large number of nuclear fuels have been consumed in the reactor. The HPTWR with nonuniform radial fuel arrangement has the axial and radial breeding waves in the depletion process (see Section 3.2) and thus has a higher breeding capability relative to optimized HPTWR. Although the initial k_{eff} of HPTWR with nonuniform radial fuel arrangement is slightly less than that of optimized HPTWR (1.0018), the highest k_{eff} of HPTWR with nonuniform radial fuel arrangement in the depletion process is higher than that of optimized HPTWR (1.0068) [7]. The lifetime of HPTWR with nonuniform radial fuel arrangement is about 50 years, which is 4 years longer than that of optimized HPTWR (46 years) because of its higher breeding capability. Besides, the burnup of HPTWR with nonuniform radial fuel arrangement is about 106.14 GWd/MTU at EOC, which is higher than that of optimized HPTWR (96.02 GWd/MTU) [7].

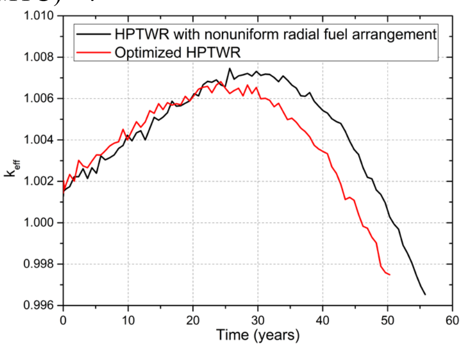

Fig.2 Time profiles of k_{eff} for HPTWR with nonuniform radial fuel arrangement and optimized HPTWRs.

The nuclear fuel will be continuously consumed in the HPTWR with nonuniform radial fuel arrangement to maintain the power output by the chain fission reactions. Besides, ^{239}Pu and ^{241}Pu will be accumulated in the reactor by the neutron capture and decay reactions of ^{238}U. For the HPTWR with nonuniform radial fuel arrangement, Fig.3 shows the consumed ^{235}U and ^{238}U, and produced ^{239}Pu and ^{241}Pu masses during the whole reactor operation. The ^{235}U and ^{238}U masses in the reactor gradually decrease due to the neutron capture and fission reactions. Therefore, the consumed ^{235}U and ^{238}U masses in the reactor are continuously increased to about 0.88 t and 1.41 t respectively. The increase rate of consumed ^{235}U mass continuously decreases during operation because the new produced fissile ^{239}Pu and ^{241}Pu masses in the reactor are continuously increased and can provide a positive reactivity in the reactor. The produced ^{239}Pu mass in the reactor is increased to about 0.69 t at EOC. The corresponding increase rate continuously decrease during the reactor operation because of the decrease of ^{238}U inventory. The produced ^{241}Pu mass in the reactor is increased to about 3.39 kg at EOC. The corresponding increase rate continuously increase in the reactor because of the increase of ^{239}Pu inventory. Table 3 shows the consumed ^{235}U and ^{238}U, and produced ^{239}Pu and ^{241}Pu masses for the HPTWR with nonuniform radial fuel arrangement and optimized HPTWR at EOC. Due to it longer lifetime of reactor, the consumed mass of nuclear fuel and produced mass of fissile nuclides in the HPTWR with nonuniform radial fuel arrangement are higher than those in the optimized HPTWR.

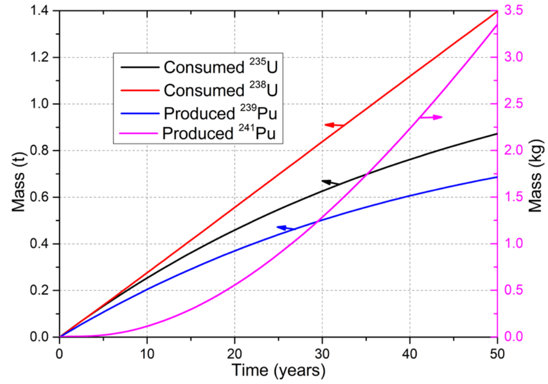

Fig.3 Time evolutions of consumed ^{235}U and ^{238}U, and produced ^{239}Pu and ^{241}Pu masses in HPTWR with nonuniform radial fuel arrangement

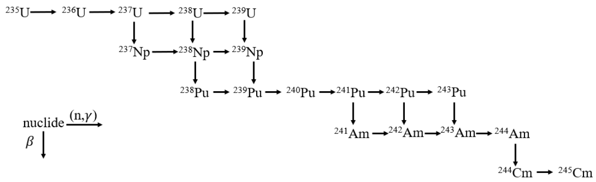

Fig.4 Simplified depletion chains for actinides.

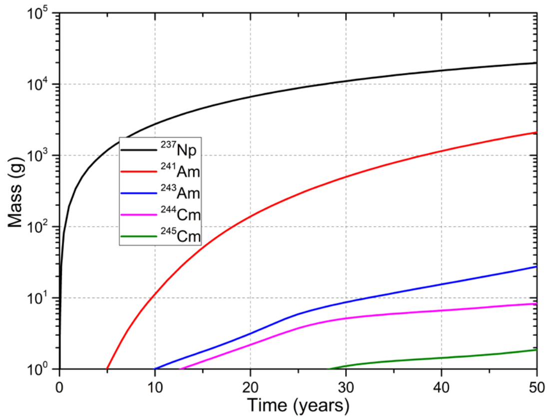

Fig.5 Time evolutions of produced MAs in HPTWR with nonuniform radial fuel arrangement.

Table 3 Consumed ^{235}U and ^{238}U, and produced ^{239}Pu and ^{241}Pu masses for HPTWR with nonuniform radial fuel arrangement and optimized HPTWR at EOC

Mass	Consumed ^{235}U (tons)	Consumed ^{238}U (tons)	Produced ^{239}Pu (tons)	Produced ^{241}Pu (kg)
HPTWR with nonuniform radial fuel arrangement	0.88	1.41	0.69	3.39
Optimized HPTWR	0.81	1.29	0.65	2.90

Table 4 Produced MAs masses for HPTWR with nonuniform radial fuel arrangement and optimized HPTWR at EOC

Produced mass	^{237}Np (kg)	^{241}Am (kg)	^{243}Am (g)	^{244}Cm (g)	^{245}Cm (g)
HPTWR with nonuniform radial fuel arrangement	19.96	2.15	28.1	8.35	1.89
Optimized HPTWR	17.88	1.66	20.0	7.43	1.61

Besides, the lifetime of HPTWR with nonuniform radial fuel arrangement is about 50 years, which will accumulate many minor actinides (MAs) in the reactor by the chain neutron capture and decay reactions. The MAs are the high-level radioactive nuclides, whose accumulation will cause potential radiological hazards to the biosphere [16]. The main MAs in the traveling wave reactor consist of ^{237}Np, ^{241}Am, ^{243}Am, ^{244}Cm and ^{245}Cm. Fig.4 shows the production chain of MAs. Fig.5 shows the produced MAs masses in the HPTWR with nonuniform radial fuel arrangement during the reactor operation. The longer production chain will spent the longer time to accumulate the MAs in the reactor. Therefore, the produced ^{37}Np, ^{241}Am, ^{243}Am, ^{244}Cm and ^{245}Cm masses in the HPTWR with nonuniform radial fuel arrangement decrease in turn. The produced ^{37}Np, ^{241}Am, ^{243}Am, ^{244}Cm and ^{245}Cm masses are about 19.96 kg, 2.15 kg, 28.1 g, 8.35 g and 1.89 g at EOC respectively. Table 4 shows the produced MAs masses for HPTWR with nonuniform radial fuel arrangement and optimized HPTWR at EOC [7]. Due to it longer lifetime of reactor, the produced MAs in the HPTWR with nonuniform radial fuel arrangement are higher than those in the optimized HPTWR.

3.2 Power distribution

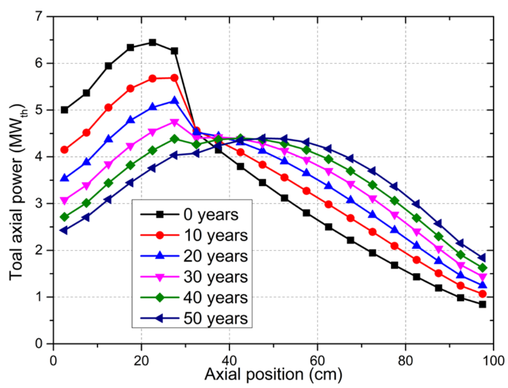

Fig.6 Total axial power profiles for HPTWR with nonuniform radial fuel arrangement

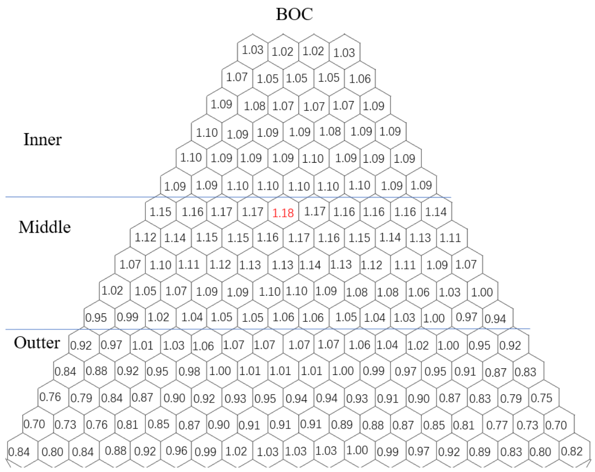

Fig.7 Normalized radial power profile of 1/6 core for HPTWR with nonuniform radial fuel arrangement at BOC.

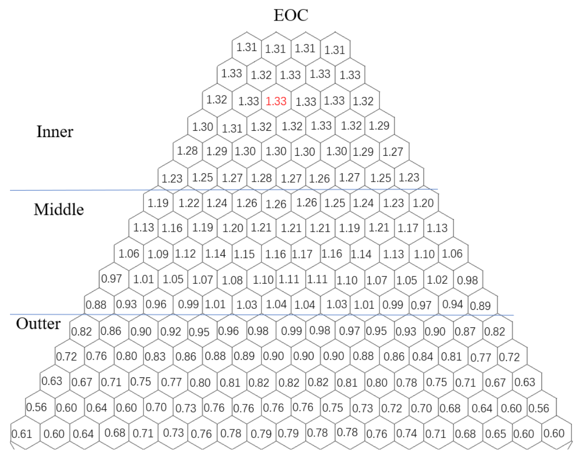

Fig.8 Normalized radial power profile of 1/6 core for HPTWR with nonuniform radial fuel arrangement at EOC.

To investigate the propagation of axial neutron traveling wave, Fig.6 shows the total axial power distribution of the HPTWR with nonuniform radial fuel arrangement during operation. The axial power peak is in the ignition fuel region at BOC because it has a higher average ^{235}U enrichment relative to the breeding fuel region. The power peak, total powers of ignition and breeding fuel regions are about 6.45 MW$_{th}$, 39.87 MW$_{th}$ and 30.13 MW$_{th}$ at BOC respectively. Due to the consumption of ignition fuel region and breeding of breeding fuel region, the power distributions of ignition and breeding fuel regions continuously decrease and increase during the reactor operation respectively. The power peak is transferred to the breeding fuel region at about 40 years. Because the power distribution of breeding fuel region gradually increases, the axial power peak is decreased to about 4.40 MW$_{th}$ at EOC, which can reduce the hot spot factor and improve the safety of reactor. The axial position of total power peak is propagated from the axial location of 22.5 cm at BOC to 47.5 cm at EOC. The corresponding propagating velocity of the total axial power peak is about 0.4902 cm/years. The traveling wave velocity of the total axial power peak in the HPTWR with nonuniform radial fuel arrangement is less than that in the optimized HPTWR (0.5435 cm/years) [7] because it has also a radial traveling wave.

Fig.7 and Fig.8 shows the corresponding normalized radial power distributions of 1/6 core for the HPTWR with nonuniform radial fuel arrangement at BOC and EOC respectively. Although the enrichment of ^{235}U in the radial outer fuel region is higher than that in the radial middle fuel region, the average power of fuel element in the radial middle fuel region is higher than that in the outer fuel region because a part of neutrons in the radial outer fuel region are leaked to the reflector during the reactor operation. Therefore, the highest power fuel element is in the radial middle fuel region and about 1.18 at BOC. The radial middle fuel region has a higher average power fuel element relative to the radial inner fuel region. More ^{238}U in the radial inner fuel region will transformed into fissile ^{239}Pu and ^{241}Pu by capturing the neutrons leaked from the middle fuel region during the reactor operation. Therefore, the power of fuel element in the radial inner fuel region is increased. Besides, the power of outer fuel element is decreased during operation because of the more neutron leakage. Therefore, the highest power fuel element is propagated to the radial inner fuel region at EOC.

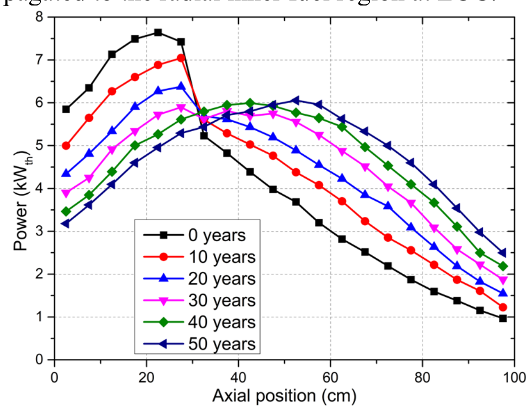

Fig.9 Axial power profiles of highest power fuel element for HPTWR with nonuniform radial fuel arrangement.

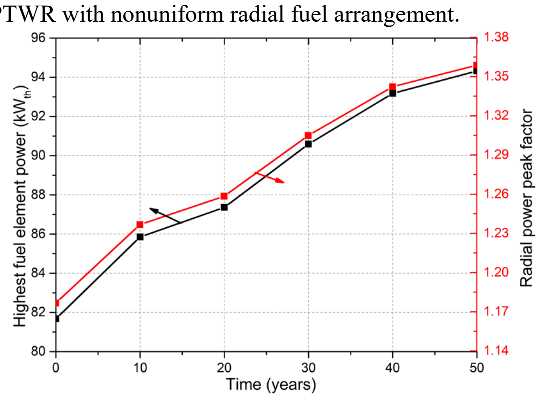

Fig.10 highest fuel element power and radial power peak factor for HPTWR with nonuniform radial fuel arrangement during reactor operation.

Fig.9 shows the axial power distribution of the highest power fuel element in the HPTWR with nonuniform radial fuel arrangement during operation. Fig.10 shows the corresponding total power of highest power fuel element and the corresponding radial power peak factor. The power peak of highest fuel element is also be propagated from the ignition fuel region at BOC to the breeding fuel region at EOC. The corresponding axial positions of power peak in the highest fuel element at BOC and EOC are 22.5 cm and 52.5 cm respectively. The corresponding propagating velocity is about 0.5582 cm/years, which is higher than that in the total axial power distribution because of its higher power output. Besides, the total power of highest power fuel element is about 81.68 kW$_{th}$ at BOC in the HPTWR with nonuniform radial fuel arrangement, which is less than that in the optimized HPTWR (96.16 MW$_{th}$) [7] because the reactor is divided into three fuel regions in the radial direction. The corresponding radial power peak factor is decreased to about 1.18 at BOC. Because the HPTWR with nonuniform radial fuel arrangement has a higher breeding capability, the total power of highest power fuel element and radial power peak factor are increased to about 94.32 kW$_{th}$ and 1.358 at EOC respectively. Both the increase rates of the total power of highest power fuel element and radial power peak factor gradually decrease during the reactor operation because of the consumption of the fuel element.

3.3 Thermal analyses

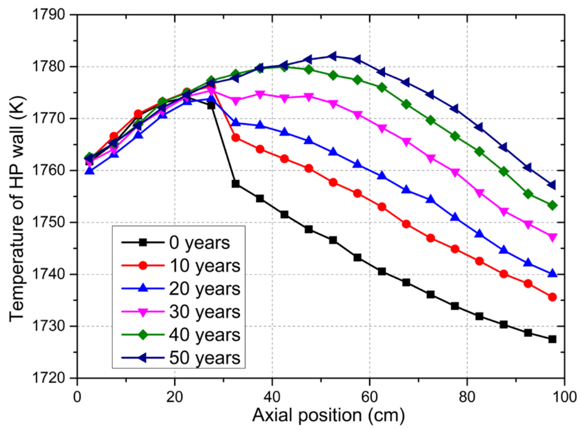

Fig.11 Temperature distribution of HP wall in highest power fuel element of HPTWR with nonuniform radial fuel arrangement during reactor operation.

Fig.11 shows the temperature distributions of HP wall in the highest power fuel element of HPTWR with nonuniform radial fuel arrangement during operation. Fig.12 shows the temperature peak of HP wall and corresponding axial position of temperature peak. The highest temperature of HP wall is about 1774.1 K at BOC. The temperature peaks of HP wall has a small fluctuation during the first 30 years operation because the temperature of HP wall is always in the axial ignition fuel region. Then, the temperature peak of HP wall has a quick increase during the next operation because the temperature peak of HP wall is transferred to the axial breeding fuel region. The temperature peak of HP wall is increased from about 1774.12 K at BOC to about 1782.02 K at EOC because of the increase of the total power of highest power fuel element during operation. The temperature distributions of HP wall in the ignition fuel region and breeding fuel region have a small change and large increase during the reactor operation respectively because of the propagation of axial and radial neutron breeding waves. The corresponding axial position of temperature peak is transferred from 22.5 cm at BOC to 52.5 cm at EOC.

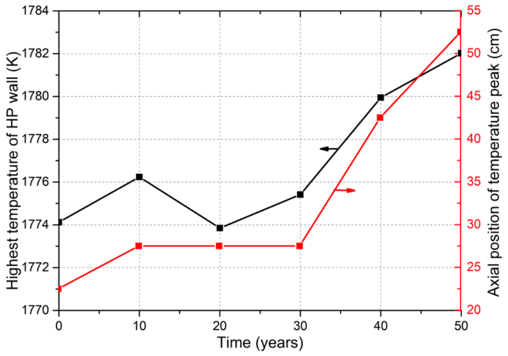

Fig.12 Highest temperature and axial position of HP wall in highest power fuel element of HPTWR with nonuniform radial fuel arrangement during reactor operation.

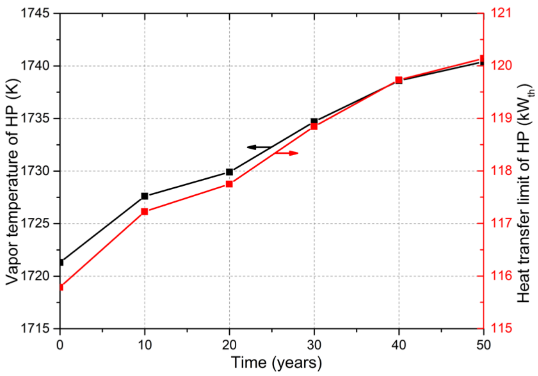

Fig.13 Vapor temperature and heat transfer limit of HP in highest power fuel element of HPTWR with nonuniform radial fuel arrangement during reactor operation.

Fig.13 shows the vapor temperature and corresponding heat transfer limit of HP in the highest power fuel element of the HPTWR with nonuniform radial fuel arrangement during operation. The formulations of the four limits for Li HP can be found in our previous work [7]. Besides, Fig.14 shows the corresponding thermal transfer margin of HP in the highest power fuel element. The vapor temperature of HP in the highest power fuel element is mainly decided by its total fission power. Therefore, the corresponding vapor temperature of HP in the highest power fuel element is increased from about 1721.3 K at BOC to about 1740.4 K at EOC. The corresponding heat transfer limit is increased from about 115.78 K at BOC to about 120.14 K at EOC. Therefore, the heat transfer margin is gradually decreased during the whole operation. The heat transfer margin of HP in the highest power fuel element is always higher than 21.4% during the whole operation, which provides a good safety advantage to ensure operation of reactor.

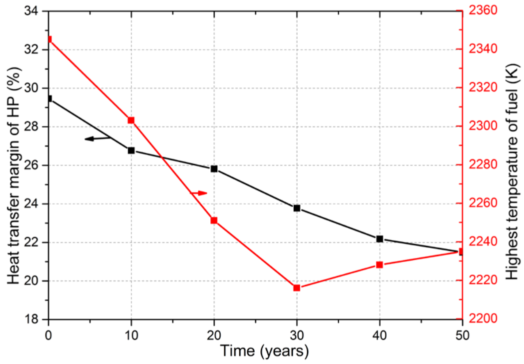

Fig.14 Heat transfer margin of HP and highest temperature of fuel in highest power fuel element of HPTWR with nonuniform radial fuel arrangement during reactor operation.

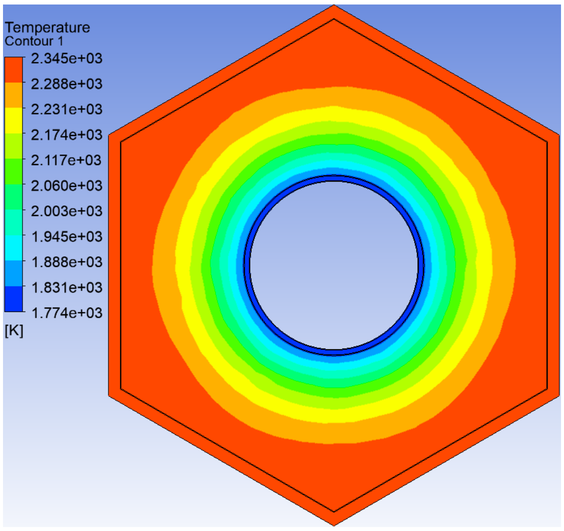

Fig.15 Radial temperature distribution in the fuel element with highest power of HPTWR with nonuniform radial fuel arrangement at BOC.

The highest operation temperatures of fuel element in the highest power fuel element of HPTWR with nonuniform radial fuel arrangement is calculated by the FLUENT. The fuel element is equally divided into 20 smaller zones in the axial direction in the calculations as the same in neutronics calculation and thermal analysis of HP. The axial and radial boundaries of per small zone fuel element are assumed to be adiabatic in the calculations. The thermal conductivities of UN fuel are set to be 30 W/(m·K) at 2200 K. The mesh independence analysis of the FLUENT model has been calculated in our previous work [7]. Fig.15 shows the cross-section temperature distribution of small zone fuel element with highest power in the axial middle position. The temperature of UN fuel gradually increases with the increase of radius in the fuel element because the fuel element has a central HP. Fig.14 shows the highest temperature of fuel in the highest power fuel element during the reactor operation. The highest operation temperature of UN fuel is about 2345 K at BOC and then decreases to about 2216 K at 30 years because the axial power distribution has a flattening. Then, the highest operation temperature of UN fuel is increased to about 2235 K at EOC because the axial power distribution flattening has a relatively small change and the power peak of highest power fuel element is increase from 5.90 kW_{th} at 30 years to about 6.05 kW_{th} at EOC.

Both the highest operation temperatures of HP wall and UN fuel at BOC are decreased from about 1800 K and 2394 K to about 1774 K and 2345 K at BOC when the optimize HPTWR is divided into fuel regions in the radial direction [7]. At EOC, the highest operation temperatures of HP wall and UN fuel in the HPTWR with nonuniform radial fuel arrangement (about 1782 K and 2235 K) are approximately consistent with results in the optimized HPTWR (about 1784.6 K and 2234 K) respectively. The optimize HPTWR with three radial fuel regions can decrease the highest operations of HP wall and fuel during operation.

4. Conclusions

In this work, the optimized HPTWR is divided into three fuel regions in the radial direction to reduce the highest operate temperature of UN fuel and HP wall. The lifetime, velocity of axial power peak, highest operate temperature of the reactor are discussed. The conclusion obtained can be summarized as follows:

1.The HPTWR with nonuniform radial fuel arrangement has a higher breeding capability relative to optimized HPTWR because it has a radial and axial neutron breeding wave. The 70 MW_{th} HPTWR with nonuniform radial fuel arrangement can continuously operate about 50 years without refueling with the 0.7% variation (swing) range of k_{eff}. The consumed ^{235}U and ^{238}U, and produced ^{239}Pu and ^{241}Pu masses in the reactor are continuously increased to about 0.88 t, 1.41 t, 0.69 t and 3.39 kg at EOC respectively. The produced ^{37}Np, ^{241}Am, ^{243}Am, ^{244}Cm and ^{245}Cm masses are about 19.96 kg, 2.15 kg, 28.10 g, 8.35 g and 1.89 g in the spent fuel at EOC respectively.

2.The propagation velocity of the total axial power peak of the HPTWR nonuniform radial fuel arrangement is about 0.4902 cm/years. The radial power peak factor of the HPTWR nonuniform radial fuel arrangement is decreased to 1.18 relative to the optimized HPTWR (1.36). The total power of highest power fuel element is increased from about 81.68 kW_{th} at BOC to about 94.32 kW_{th} at EOC. The highest power fuel element is transferred from the radial middle fuel region at BOC to the inner fuel region at EOC.

3.The temperature peak of HP wall in the highest power fuel element is increased from about 1774.12 K at BOC to about 1782.02 K at EOC. The heat transfer margin is always higher than 21.4% during the whole operation. The highest operation temperature of UN fuel is about 2345 K at BOC and then decreases to about 2235 K at EOC.

Acknowledgement

The authors thank the National Natural Science Foundation of China for their support through Grant No. 11205098.

REFERENCES

[1] Wang, D., Yan, B., Chen, J., 2020. The opportunities and challenges of micro heat piped cooled reactor system with high efficiency energy conversion units. Ann. Nucl. Energy 149, 107808.
[2] Yan, B., Wang, C., Li, L., 2020. The technology of micro heat pipe cooled reactor: A review. Ann. Nucl. Energy 135,106948
[3] Niederauer, G., Lantz, E., 1970. A split-core heat-pipe reactor for space power applications. NASA TM X-52918, 2.
[4] McClure, P., Poston, D., Rao, D.V., et al., 2015. Design of Megawatt Power Level Heat Pipe Reactors. LA-UR-15-28840.
[5] Westinghouse Electric Company, 2017. Westinghouse EVinci TM Micro Reactor. Accessed July 2018.
[6] Ma, K., Hu, P., 2022. Preliminary conceptual design and neutroncis analysis of a heat pipe cooled traveling wave reactor. Ann. Nucl. Energy 168, 108907.
[7] Ma, K., Hu, P., 2023. Preliminary neutronics and thermal analysis of a heat pipe cooled traveling wave reactor. Ann. Nucl. Energy 190, 109876.
[8] Alawneh, L.M., Vaghetto, R., Hassan, Y., 2022. Conceptual design of a 3 MWth yttrium hydride moderated heat pipe cooled micro reactor. Nuclear Engineering and Design 397, 111931.
[9] El-Genk. M.S., Tournier. J.M., Conceptual Design of HP-STMCs Space Reactor Power System for 110 kWe. AIP Conference Proceedings 699, 658 (2004)
[10] Wang, K., Li, Z., She, D., et al., 2015. RMC- A Monte Carlo code for reactor core analysis. Ann. Nucl. Energy 82, 121–129.
[11] Ma, Y., Liu, S., Luo, Z., et al., 2019. RMC/CTF multiphysics solutions to VERA core physics benchmark problem 9. Ann. Nucl. Energy 133, 837–852.
[12] Chadwick, M.B., Obložinský, P., Herman, M., et al, 2006. ENDF/B-VII.0: Next Generation Evaluated Nuclear Data Library for Nuclear Science and Technology. Nuclear data sheets 107, 2931-3059.
[13] Huang, J., Han, J., Cai, X., et al., 2015. Breed-and-burn strategy in a fast reactor with optimized starter fuel. Prog. Nucl. Energy 85, 11–16.
[14] Shrestha, R., Rizwan-uddin., 2014. Modeling space–time evolution of flux in a traveling wave reactor. Ann. Nucl. Energy 70, 90-95.
[15] Uda, N., Miyazawa, A., Inoue, S., et al., 2012. Forced Convection Heat Transfer and Temperature Fluctuations of Lithium under Transverse Magnetic Fields. Journal of Nuclear Science and Technology. 38, 11.
[16] Ma, K., Hu, P., 2023. Analysis of UO_2 , UN and U–10Zr fuels burning in a MegaPower reactor with solid monolithic and independent fuel element core designs. Prog. Nucl. Energy. 162, 104773.